Relaxation Constant in the Folding of Thin Viscoelastic Sheets

Kasra Farain*

Department of Physics, Sharif University of Technology, P.O. Box 11155-9161, Tehran, Iran

(Received 20 August 2019; revised manuscript received 28 October 2019; published 17 January 2020)

If one folds a thin viscoelastic sheet under an applied force, a line of plastic deformation is formed that shapes the sheet into an angle. This study determines parameters that define this angle and shows that, no matter how much load one applies, it is impossible to make angles less than a certain minimum angle in a definite time. Moreover, it is shown that regardless of whether the sheet is released freely afterward or kept under load, a logarithmic relaxation process follows the first deformation. The slope of this logarithm is the same in both conditions and depends neither on the applied force nor on the thickness of the sheet, which indicates that it is directly a probe of the molecular mobility of the material. This intrinsic relaxation constant is measured at approximately 0.1 and 6 for Mylar and paper sheets, respectively. It is also suggested that the observed minimum angle of folding can be defined as a characteristic index for the plasticity of different materials.

DOI: 10.1103/PhysRevApplied.13.014031

I. INTRODUCTION

Folding is at first sight a seemingly trivial way of making multilayer stacks or three-dimensional objects from thin sheets. However, folding problems arise in a variety of living systems. For example, the shape of viral shells is determined by the energies of folding [1,2], the folds of an earwig insect's wing allow it to change shape and lock into specific geometries [3], and cerebral-cortex expansion occurs with increasing degrees of folding of the cortical surface [4]. Folding has also artistic and technological applications. In the decorative arts and fashion, creasing properties of sheets or fabrics, i.e., crease resistance and recovery, are crucial for designers [5]. In space technology, it is important to design solar panels with the ability to change between folded stowed and planar configurations in an optimized way [6]. More recent technological applications of folding are related to the next-generation soft robots [7,8] and wearable electronics [9], which include thin two-dimensional elastomeric parts that undergo continual bending and folding during use. An understanding of the structural and geometrical changes, the force production, and the nonlinear and time-dependent responses, of these folding parts is enormously important for their precise and efficient control, especially when small forces are exploited [10]. Lastly, origami designed structures [11–14] and crumpled sheets [15–17], which have recently attracted a great deal of attention, are composed, respectively, of ordered and random networks of creases created in a sheet. The mechanical properties of such systems are determined by not only the network but also by the response of each of the building block creases, which can be considered as elastic hinges of specific stiffness connecting flexible panels [18].

In this research, the folding of thin viscoelastic sheets and the subsequent slow relaxation of the remaining plastically deformed creases are studied. Imagine a piece of paper bent gently and put under some slowly increasing force, similar to Fig. 1(a). The elastic energy of bending, first spread smoothly throughout the curved region, suddenly concentrates in a strongly bent edge [19]. In other words, at some point the maximum stress passes the yield point of the material and triggers a noncontinuous self-accelerating process (the geometry of the applied force), which causes permanent changes in the structure. A viscoelastic polymer, when subjected to an applied stress, shows a combination of time-dependent irreversible viscous flow and immediate recoverable elastic strain [20,21]. When a crease is created in a viscoelastic sheet after pressing by a certain load for a short time interval, the irreversible viscous flow continues under the effect of the elastic response even after releasing. This is, in a sense, a perturbation in a disordered molecular system that relaxes toward an equilibrium (or quasiequilibrium) state over several hours [22]. Similar slow relaxations have been observed in a wide variety of out-of-equilibrium disordered systems, such as glassy polymers below the glass-transition temperature [23,24], amorphous metals [25–27], granular media [28,29], frictional interfaces [30], crumpled sheets [16,31], and electron glasses [32]. Apart from the theoretical implications, due to their vast use in technology, slow time-dependent structural or geometrical changes are particularly important in the case of polymer glasses. Here, in addition to presenting

*kfarain@seas.harvard.edu

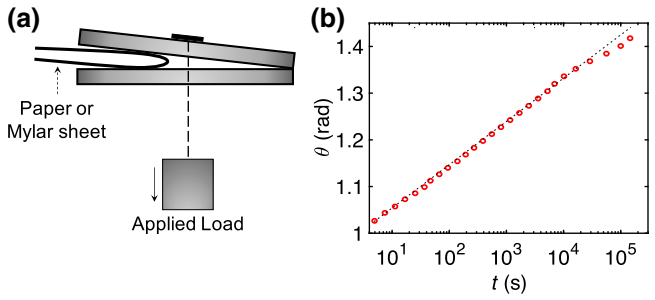

FIG. 1. (a) A schematic of the fold-preparation setup. The crease is created by applying a constant load on a folded sheet for a given time (3 s for most of the experiments). (b) The time evolution of the angle of a typical crease in the 0.25-mm-thick Mylar sheet. The crease has been unloaded at $t = 0$.

a thorough phenomenological description of folding using Mylar sheets, I introduce a simple and fast way to perturb a polymer glass to an out-of-equilibrium state, which is followed by a robust logarithmic relaxation. The time origin of this logarithm corresponds to the perturbation time. Moreover, it is shown that, independent of the folding parameters and the external geometrical constraints on the fold afterward, the logarithmic process evolves with a constant rate that is a characteristic of the material. The slopes of similar logarithmic changes are widely used to compare the recovery dynamics of polymers [33].

II. EXPERIMENTAL

Commercial Mylar sheets of different thicknesses of 0.08, 0.10, 0.17, and 0.25 mm are cut into 15 mm × 25 mm rectangles. These pieces are then bent smoothly by hand along the short edge (the crease length of $L = 15$ mm) and pressed under defined forces between two flat metallic plates for 3 s. The plates are hinged at one side, which guarantees that all the force is concentrated on the crease line when they are closed [Fig. 1(a)]. Moreover, to avoid any extra shock to the folded edge, the plates are closed slowly, using a handle. After releasing, the folded pieces settle at an initial angle instantly and then, as also observed by others [22], start to unfold in a perfect logarithmic way over several hours [Fig. 1(b)]. One side of the samples is held by a gripper and the other side can open freely, parallel to the ground. The samples are illuminated from the side and observed with a camera. The images are processed using ImageJ [34] or a custom-made program in MATLAB.

III. RESULTS AND DISCUSSION

The logarithmic unfolding can be expressed by the following equation:

$$\theta = a \log(t - t_0) + b, \tag{1}$$

where a and b are constants and t_0 corresponds to the instant at which the crease is unloaded. Given knowledge of the logarithmic dependence of the angle on $t - t_0$, t_0 can also be extracted from the unfolding data within an accuracy of a few seconds. This means that by simply observing the relaxation of a folded sheet, one can determine when the folding has happened. However, it should be pointed out that the logarithmic relationship is not valid in the immediate vicinity of t_0, as it diverges. Additionally, more waiting in the loading stage will lead to a larger deviation from the logarithmic behavior in the starting seconds, as previously reported by Thiria and Adda-Bedia for the relaxation of the force produced by a creased sheet [22]. The small deviation in the linear behavior after 2×10^4 s in Fig. 1(b) probably happens when the generated force in the creased region is comparable with other mechanisms such as vibrations in the system. This deviation starts after approximately 10^3 s, when the direction of the sample is such that the gravitational force is also working on the system. The discussion presented here may also help one to understand the relaxation behavior of crumpled sheets, which consist of a random pattern of creases with different ages and strengths through consecutive crumpling at different times [16].

A. Minimum angle of folding

When one folds a sheet of paper in two, the fold edge is usually pressed strongly to minimize the return of the second layer. But to what extent does this extra pressing help? Figure 2(a) shows the crease angle in the folded Mylar pieces of different thicknesses as a function of the load acting on them, $t_i = 3$ s after folding. At first, the obtained angle decreases logarithmically with the applied load. Then, it reaches a limit angle and further increasing of the load no longer affects the crease. In fact, at some point, the top and bottom Mylar layers are completely compressed against each other and the extra load just increases the normal stress on the layers. Therefore, it is not possible to make angles less than a certain minimum angle in the Mylar sheets by applying larger loads. Additionally, all the four curves for different thicknesses of Mylar finally converge to the same limit angle. This can be understood by the following argument. Suppose that the sheet thickness h is doubled and the compressive force F is increased correspondingly so that the limit angle is obtained again. This does not alter the form of the strain profile in the semicircular cross section at the ridge, which defines the fold angle. In other words, only the value of h with respect to F is important and there is no other scale in the experiment.

B. Dependence of fold angle on sheet thickness

From the elasticity theory for small deflections of thin plates, we know the bending rigidity as $B = Eh^3/$

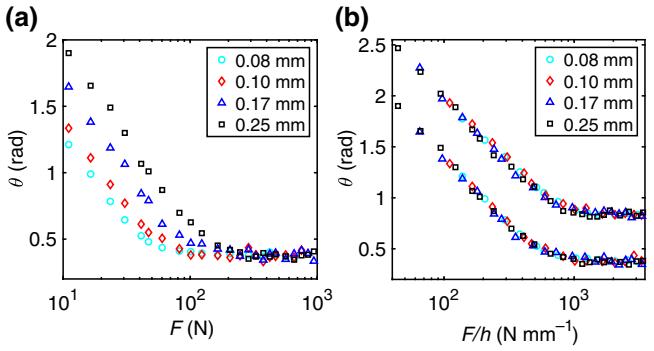

FIG. 2. (a) The crease angle of Mylar sheets with four different thicknesses, $t_i = 3$ s after folding, as a function of the applied force. All the curves finally converge into the same limit angle. (b) The angle of the folded sheets at $t_i = 3$ s (lower curve) and $t_f = 48$ h (upper Curve) plotted as a function of the applied force normalized by the thickness of the sheets. The data points for the different thicknesses collapse onto each other. The vertical distance between the t_i and t_f curves remains constant throughout the logarithmic and saturation (after 10^3 N mm^{-1}) parts.

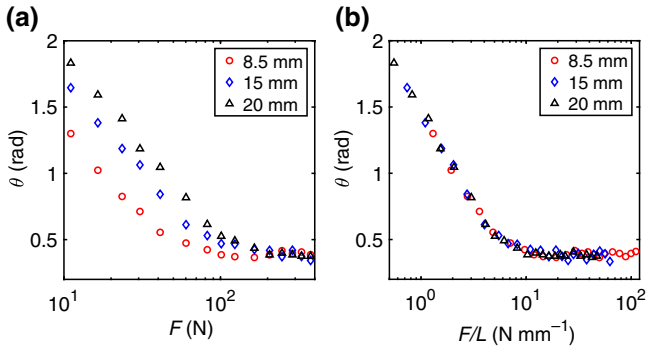

FIG. 3. (a) The crease angle of 0.17-mm-thick Mylar pieces at $t_i = 3$ s as a function of the applied pressing force for three different lengths of the crease, 8.5, 15, and 20 mm. (b) The data collapse onto each other when plotted as a function of the applied force per unit length of the crease.

$12(1-\nu^2)$, where h, E, and ν are the thickness of the plate, the modulus of elasticity, and the Poisson ratio, respectively [35]. Considering the bending rigidity as the moment per unit length of the crease per unit of curvature $Fh/[L(1/h)]$ and comparing it with the above expression, one can expect $F/(LhE)$ to be the relevant dimensionless quantity for describing the angle caused by folding. The lower curve in Fig. 2(b) shows the data of Fig. 2(a) when the applied load is scaled by the thicknesses of the sheets. This plot confirms that the folding force appears correctly as F/h in the governing relation. The upper curve in Fig. 2(b) presents the angle of the same samples after $t_f = 48$ h.

C. Relaxation constant

Knowledge of θ at two different times is enough to find the constant a and b of Eq. (1). If $\theta = \theta_i$ and θ_f at times t_i and t_f, respectively, then

$$\theta = \theta_i + \frac{\theta_f - \theta_i}{\log(t_f/t_i)} \log\left(\frac{t}{t_i}\right), \tag{2}$$

where we take $t_0 = 0$ for simplicity. Interestingly, as observed in Fig. 2(b), the lower and upper curves have the same slope and $\theta_f - \theta_i$ is a constant throughout the logarithmic regime and, with a small change, in the saturation regime (after 10^3 N mm^{-1}). Therefore, the quantity $a = (\theta_f - \theta_i)/\log(t_f/t_i)$ depends neither on the applied force nor on the thickness of the sheets. Rearranging Eq. (2) as

$$\frac{\theta - \theta_i}{\log(t/t_i)} = \frac{\theta_f - \theta_i}{\log(t_f/t_i)}, \tag{3}$$

one can see it does not depend on the specific choice of t_i and t_f either and can be regarded as a material property. For the Mylar sheets used in this work, in the logarithmic regime $a = 0.124 \pm 0.005$ and in the limiting-minimum-angle or maximum-deformation regime, $a = 0.098 \pm 0.005$ is obtained. Put concisely, up to a minimum angle, the crease angle scales with $\log(F/h)$ (which is represented by the value of θ_i), but the relaxation toward equilibrium is independent of the applied pressing force and the thickness of the sheet and happens with a constant rate (which is given by the slope a).

D. Dependence on fold length

We also examine how the folding force needed to make an angle in a sheet is related to the length of the fold. Figure 3(a) shows the angle of 0.17-mm-thick Mylar pieces of three different widths (fold lengths) of $L = 8.5$, 15, and 20 mm, at $t_i = 3$ s, versus the load acting on them.

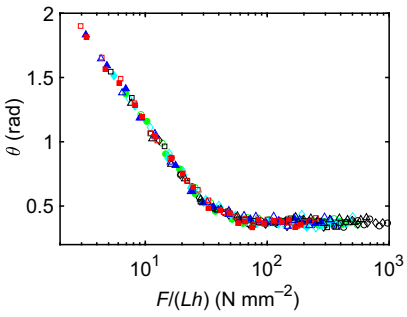

FIG. 4. The crease angle of Mylar sheets with four different thicknesses of $h = 0.08$ (circles), 0.10 (diamond), 0.17 (triangle), and 0.25 (square) mm, for three different crease lengths of $L = 8.5$ (black), 15 (colored), and 20 mm (filled colored), as a function of the applied pressing force per unit of the crease length per unit of the sheet thickness. All data points fall onto a single curve when the force is normalized as F/Lh.

In Fig. 3(b), the data collapse onto a single curve when they are plotted as a function of the force per unit length of the fold. To verify this result for other thicknesses of Mylar sheets, Fig. 4 represents the angle data corresponding to different combinations of L and h and confirms that all curves fall on top of each other for any L and h if the force is normalized as $F/(Lh)$. Therefore, the folding force for creating a certain angle in a sheet is also proportional to the length of the fold and the rescaled force $F/(Lh)$ must be used to characterize the folding. However, it should be noted that the linear proportionality between the applied load and the crease length is only captured before the saturation of the deformation.

E. Minimum fold angle as an index for plasticity

One remarkable feature of the results presented so far is that there is a minimum angle that, no matter how much load one uses, it is impossible to fold a Mylar sheet to a more acute angle than that minimum. This minimum angle, which is also independent of the thickness of the sheets and therefore is a characteristic of the material, is 50° for Mylar and, for instance, approximately 36, 118, and 0° in the case of printing paper, polyethylene sheets, and aluminum foil, respectively. These results suggest that the minimum fold angle may be utilized to define an index for plastic behavior of different materials.

F. Effect of loading time

Furthermore, the effect of the loading time on the final angle of the folded sheets is investigated. In order to do this, folded samples of given thickness and dimensions are prepared by applying a constant load over various time intervals. In Fig. 5(a), the measured angles at $t_i = 3$ s and $t_f = 48$ h (after unloading the samples) for Mylar sheets with thicknesses of 0.25 and 0.17 mm and a width (crease length) of 15 mm are plotted versus different loading times. The applied force is 40 N, which for both thicknesses falls in the logarithmic regime in Fig. 2. As observed, the crease angle also decreases logarithmically with the loading time. The slope of this logarithmic decrease is the same for both thicknesses and for the angles at $t_i = 3$ s and $t_f = 48$ h and is equal to 0.16 ± 0.02. Figure 5(b) shows the same results for Mylar sheets with thicknesses of 0.10 and 0.08 mm when the loading force is large enough to fall in the saturation regime (125 N). In this regime, the slope of the logarithmic decrease of the crease angle is 0.09 ± 0.01, which is the same as the slope of the logarithmic opening of a folded piece in the saturation regime of Fig. 2, (0.098 ± 0.005). The larger slope observed in Fig. 5(a) might be justified with the macroscopic vibrations of the top Mylar layer (due to the distance between the two layers) in the logarithmic regime of folding.

After folding, the strongly bent region has been stressed beyond the yield point and has undergone defects and

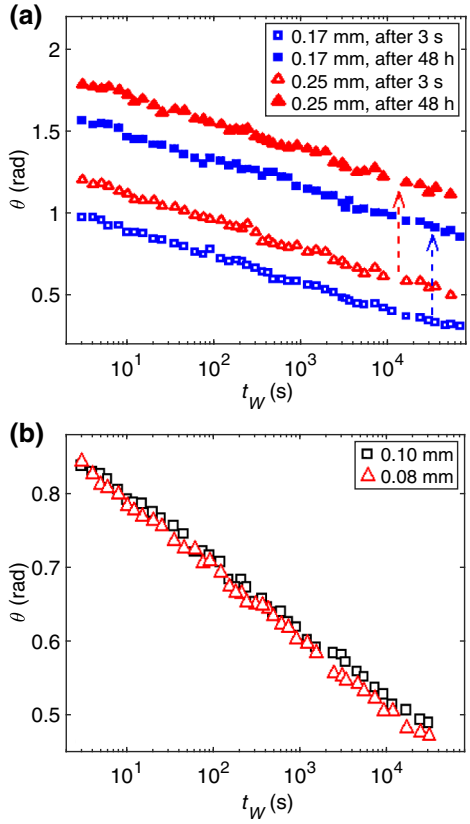

FIG. 5. The crease angle decreases logarithmically with respect to the time for which one has maintained the fold under the pressing load. (a) The crease angle as a function of the loading time, at $t_i = 3$ s and $t_f = 48$ h after removing the load, for Mylar sheets with thicknesses of 0.25 and 0.17 mm, a crease length of 15 mm, and an applied force of 40 N (which for both thicknesses falls in the logarithmic regime of Fig. 2). (b) The same as in (a), but for Mylar sheets with thicknesses of 0.10 and 0.08 mm, the angle after $t_f = 48$ h, and an applied force of 125 N (which falls in the saturation regime in Fig. 2).

sudden changes in the molecular arrangement. The new structure is out of equilibrium and immediately starts a relaxation process toward the maximum-entropy state. Moreover, this relaxation takes place toward a molecular order that is dictated by the external geometrical constraints on the sample. In Fig. 5, when the folded Mylar pieces are kept under load, the molecular activity evolves toward a state compatible with that pressed condition. After unloading, the samples continue to relax toward an equilibrium consistent with the free state. A comparison of the slope of the logarithmic unfolding and the changes in the crease angle with the loading time suggests that the relaxation mechanism is the same in both cases and does not depend on the external mechanical constraints on the system. To examine the general character of this result, we conduct the same experiments with printing paper and obtain $a = 5.7 \pm 1.5$ for the relaxation constant in both folding and unfolding tests.

IV. CONCLUSIONS

In conclusion, we study the relaxation mechanism in the folding and unfolding of thin viscoelastic sheets. In addition to describing how the crease angle changes with the thickness of the sheet, the crease length, and the magnitude, as well as the acting time of the applied pressing force, we show that after the first instantaneous plastic deformation, a slow relaxation process proceeds logarithmically. The rate of this process is the same when the sheet is freely opening or remains for longer under the pressing force and is independent of the sheet thickness and the applied force. Therefore, it is identified as a material property that can be utilized as an experimental measure for assessing the molecular mobility and the stress relaxation rate in polymer glasses. Moreover, in a given loading time, the minimum achievable fold angle is limited and constant for all thicknesses of the same material and can be a characteristic index for defining the plasticity of different materials.

ACKNOWLEDGMENTS

I would like to express my gratitude to Professor Shmuel Rubinstein of Harvard University for his support and stimulating discussions throughout this study.

[1] T. T. Nguyen, R. F. Bruinsma, and W. M. Gelbart, Continuum Theory of Retroviral Capsids, Phys. Rev. Lett. **96**, 078102 (2006).
[2] W. H. Roos, R. Bruinsma, and G. J. L. Wuite, Physical virology, Nat. Phys. **6**, 733 (2010).
[3] J. A. Faber, A. F. Arrieta, and A. R. Studart, Bioinspired spring origami, Science **359**, 1386 (2018).
[4] B. Mota and S. Herculano-Houzel, Cortical folding scales universally with surface area and thickness, not number of neurons, Science **349**, 74 (2015).
[5] R. T. Shet and A. M. Yabani, Crease-recovery and tensile-strength properties of unmodified and modified cotton cellulose treated with crosslinking agents, Text. Res. J. **51**, 740 (1981).
[6] G. W. Marks, U.S. Patent 5520747 (1996).
[7] S. Felton, M. Tolley, E. Demaine, D. Rus, and R. Wood, A method for building self-folding machines, Science **345**, 644 (2014).
[8] C. Laschi, B. Mazzolai, and M. Cianchetti, Soft robotics: Technologies and systems pushing the boundaries of robot abilities, Sci. Robotics **1**, eaah3690 (2016).
[9] W. Zeng, L. Shu, Q. Li, S. Chen, F. Wang, and X.-M. Tao, Fiber-based wearable electronics: A review of materials, fabrication, devices, and applications, Adv. Mater. **26**, 5310 (2014).
[10] Y. Liu, J. K. Boyles, J. Genzer, and M. D. Dickey, Self-folding of polymer sheets using local light absorption, Soft Matter **8**, 1764 (2012).
[11] Z. You, Folding structures out of flat materials, Science **345**, 623 (2014).
[12] M. A. Dias, L. H. Dudte, L. Mahadevan, and C. D. Santangelo, Geometric Mechanics of Curved Crease Origami, Phys. Rev. Lett. **109**, 114301 (2012).
[13] B. G.-g. Chen, B. Liu, A. A. Evans, J. Paulose, I. Cohen, V. Vitelli, and C. D. Santangelo, Topological Mechanics of Origami and Kirigami, Phys. Rev. Lett. **116**, 135501 (2016).
[14] S. Li, H. Fang, and K. W. Wang, Recoverable and Programmable Collapse from Folding Pressurized Origami Cellular Solids, Phys. Rev. Lett. **117**, 114301 (2016).
[15] S. Deboeuf, E. Katzav, A. Boudaoud, D. Bonn, and M. Adda-Bedia, Comparative Study of Crumpling and Folding of Thin Sheets, Phys. Rev. Lett. **110**, 104301 (2013).
[16] K. Matan, R. B. Williams, T. A. Witten, and S. R. Nagel, Crumpling a Thin Sheet, Phys. Rev. Lett. **88**, 076101 (2002).
[17] D. L. Blair and A. Kudrolli, Geometry of Crumpled Paper, Phys. Rev. Lett. **94**, 166107 (2005).
[18] F. Lechenault, B. Thiria, and M. Adda-Bedia, Mechanical Response of a Creased Sheet, Phys. Rev. Lett. **112**, 244301 (2014).
[19] T. A. Witten, Stress focusing in elastic sheets, Rev. Mod. Phys. **79**, 643 (2007).
[20] J. J. Aklonis, W. J. MacKnight, and M. Shen, *Introduction to Polymer Viscoelasticity* (Wiley Interscience, New York, 1972).
[21] W. D. Callister, *Materials Science and Engineering: An Introduction* (Wiley, New York, 1994).
[22] B. Thiria and M. Adda-Bedia, Relaxation Mechanisms in the Unfolding of Thin Sheets, Phys. Rev. Lett. **107**, 025506 (2011).
[23] L. C. Struik, *Physical Aging in Amorphous Polymers and Other Materials* (Elsevier, Amsterdam, 1978).
[24] D. Cangialosi, V. M. Boucher, A. Alegria, and J. Colmenero, Physical aging in polymers and polymer nanocomposites: Recent results and open questions, Soft Matter **9**, 8619 (2013).
[25] Z. T. Wang, J. Pan, Y. Li, and C. A. Schuh, Densification and Strain Hardening of a Metallic Glass under Tension at Room Temperature, Phys. Rev. Lett. **111**, 135504 (2013).
[26] A. L. Greer, Metallic glasses, Science **267**, 1947 (1995).
[27] Z. Evenson, B. Ruta, S. Hechler, M. Stolpe, E. Pineda, I. Gallino, and R. Busch, X-Ray Photon Correlation Spectroscopy Reveals Intermittent Aging Dynamics in a Metallic Glass, Phys. Rev. Lett. **115**, 175701 (2015).
[28] A. Prados and E. Trizac, Kovacs-Like Memory Effect in Driven Granular Gases, Phys. Rev. Lett. **112**, 198001 (2014).
[29] M. Pica Ciamarra, A. Coniglio, and M. Nicodemi, Thermodynamics and Statistical Mechanics of Dense Granular Media, Phys. Rev. Lett. **97**, 158001 (2006).
[30] S. Dillavou and S. M. Rubinstein, Nonmonotonic Aging and Memory in a Frictional Interface, Phys. Rev. Lett. **120**, 224101 (2018).
[31] Y. Lahini, O. Gottesman, A. Amir, and S. M. Rubinstein, Nonmonotonic Aging and Memory Retention in Disordered Mechanical Systems, Phys. Rev. Lett. **118**, 085501 (2017).

[32] A. Eisenbach, T. Havdala, J. Delahaye, T. Grenet, A. Amir, and A. Frydman, Glassy Dynamics in Disordered Electronic Systems Reveal Striking Thermal Memory Effects, Phys. Rev. Lett. **117**, 116601 (2016).

[33] J. M. Hutchinson, Physical aging of polymers, Prog. Polym. Sci. **20**, 703 (1995).

[34] See http://rsb.info.nih.gov/ij/.

[35] L. D. Landau and E. M. Lifshitz, *Theory of Elasticity* (Pergamon, New York, 1986), 3rd ed.